doi: 103969/j. issn. 0490-6756. 2016. 11. 018

二氮化铂高压结构相变,弹性和热力学性质的第一性原理计算

詹国富[1], 陈芳琴[2], 朱　俊[1], 郝彦军[1], 赵宇鑫[1], 雷慧茹[1]
(1. 四川大学物理科学与技术学院, 成都 610064; 2. 南昌大学科学技术学院, 南昌 330029)

摘　要: 运用密度泛函理论广义梯度近似方法计算了 PtN_2 在莹石结构(C1),黄铁矿结构(C2),白铁矿结构(C18),$CoSb_2$ 结构,简单六角结构(SH),简单四角结构(ST)和层状结构(LS)的结构参数,弹性性质,电子结构和热力学性质. 计算了平衡态晶格参数,体模量和它的一阶导数. 计算得到人焓表明,最稳定的结构为 C2 结构,其他的为亚稳态结构. 而在我们研究的压强范围内没有发生相变. C2 结构的态密度表明它是一种具有 1.5eV 带隙的半导体. 另外,我们还预测了杨氏模量,泊松比和各向异性因子. 弹性常数,体模量,切变模量,横向声速和剪切声速随着压强的增大而单调增大. 德拜温度,热膨胀系数和热容随压强增大而增大.

关键词: 相变; 电子结构; 弹性性质; 热力学性质; PtN_2
中图分类号: O552.4+22/O414　　**文献标识码**: A　　**文章编号**: 0490-6756(2016)06-1290-09

Phase transition, elastic and thermodynamic properties of PtN_2 under high pressure from first-principles study

ZHAN Guo-Fu[1], *CHEN Fang-Qin*[2], *ZHU Jun*[1], *HAO Yan-Jun*[1], *ZHAO Yu-Xin*[1], *LEI Hui-Ru*[1]
(1. College of Physical Science and Technology, Sichuan University, Chengdu 610065, China;
2. College of Science and Technology, Nanchang University, Nanchang 330029, China)

Abstract: The structural, elastic, electronic and thermodynamic properties of PtN_2 have been studied in fluorite (C1), pyrite (C2), marcasite (C18), $CoSb_2$, simple hexagonal (denoted SH hereafter), simple tetragonal (denoted ST hereafter) and Layer structure (hereafter denoted as LS) phase by performing *ab initio* calculations within the generalized gradient approximation (GGA). The equilibrium lattice parameters, bulk modulus and its pressure derivative are in agreement with the available theoretical results and experimental data. The most stable structure is C2 phase through calculating the enthalpy, while the others are metastable. It is noted that no phase transition occurs between difference phases in the pressure range studied here. The density of states indicates that C2-PtN_2 is semiconductor with a band gap of 1.5 eV. The Young's modulus, Poisson's ratio and anisotropy factor have been predicted. We note that the elastic constant, bulk modulus, shear modulus, compressional and shear wave velocity increase monotonically with increasing pressure. The Debye temperature, thermal expansion and heat capacity increase with pressure.

Keywords: Phase transition; Electronic structure; Elastic properties; Thermodynamic properties; PtN_2

收稿日期: 2015-05-15
作者简介: 詹国富(1988－), 男, 主要从事超硬材料物理性质的研究.
通讯作者: 陈芳琴. E-mail: 56443817@qq.com; 朱俊. E-mail:zhunjun@scu.edu.cn

1 Introduction

The transition metal nitrides with unique properties in durability and conductivity have attracted special attention[1-2], since the first successful synthesis of platinum nitride at high pressures and temperatures in 2004, making it possible the design of entirely new materials such as coatings materials, thin film resistors, integrated circuits[3-5] and so on. Though, a series of theoretical and experimental efforts have been made to study their elastic properties and electronic structures[6-11], less attention has been paid to their phase transition and thermodynamic properties which are essential for further basic research and applications, especially under high pressures.

Through experimental synthesis, Crowhurst *et al*.[1] found that the lattice constant $a = 4.80$? in C2 structure. The elastic properties and electronic structure of the C2-PtN_2 were studied using the full-potential linearized augmented plane-wave (LAPW)method with the density-functional theory (DFT) by Yu *et al*.[12], and the PtN_2(C2)was semiconducting having an indirect band gap. Chen *et al*.[13] found the PtN_2 (C2) was mechanically and dynamically stable and the formation energy of C2 structure was 0.637 eV per formula unit for the nitrides. Soto[14] made a comparative analysis of heavy-metal per nitrides using self-consistent computational methods and found the bulk modulus of Pa 3(_) space group was 326 GPa. Using first-principles, Gou et al.[15] found that the PtN_2 in C2 and C18 phase were semiconducting materials through and the PtN_2(C2) were more energetically stable under the ambient condition. The elastic properties of C2-PtN_2 under high pressures have been investigated by Fu *et al*.[16] by using norm-conserving pseudopotentials with the local density approximation (LDA). The thermodynamic stabilities of various phases of the nitrides of the platinum-metal elements were systematically studied using DFT by ? berg et al.[17], which had shown the PtN_2 simple tetragonal structures at 17 GPa were thermodynamically stable with respect to phase separation. Recently, a new phase Layer structure (space group Pmmm: No. 47)has been studied about the mechanical and dynamical stability by Fan *et al*.[18] However, the phase transition and elastic properties(e.g. bulk modulus, shear modulus, Young's modulus, compressional and shear wave velocities, elastic anisotropic factor) under high pressure have seldom been reported.

In this work, We focus on phase transition, electronic structure, elastic constants under high pressures and thermodynamic properties of PtN_2 with DFT based on the linear combination of atomic orbital. This paper will be organized as follows: the theoretical method will be declared in section 2. The calculated results will been given in section 3 as well as some discussions as compared with previous results. Section 4 is the conclusions.

2 Theoretical methods

2.1 Total energy calculation

The total energy electronic structure calculation grounded on the DFT were performed within GGA using the Perdew-Burke-Ernzergof (PBE)[19] for the exchange-correlation energy in the Spanish Initiative for Electronic Simulations with Thousands of Atoms (SIESTA) code.[20-21] The total energy and atomic forces is calculated using a linear combination of atomic orbital. The finite range pseudoatomic orbital (PAOs) of the Sanky-niklewsky type[22] is generalized to include multiple-zelta decays. The interactions between electrons and core ions are simulated with the separable Troullier-Martins[23] norm-conserving pseudotentials. Pseudoatomic are performed for Pt $5d^9 6s^1$ and N $2s^2 2p^3$. All atoms are allowed to relax until atomic forces are less than 0.04 eV/?. The cut-off energy are taken to be 700 eV for C1, 800 eV for C2, 700 eV for C18. For the Brillouin zone k-point sampling, we use the $19 \times 19 \times 19$ Monkhorst-Pack[24] for C1, $11 \times 11 \times 11$ forC2, $20 \times 20 \times 20$ for C18 structure, respectively. With these parameter, the self-consistent convergence

of the total energy is less than 0.1 meV/atom for PtN_2.

2.2 Elastic constants

We calculate the second derivatives of the internal energy with respect to the strain tensor in order to obtain the elastic constants. The theoretical method proposed by Sin′ko and Smirnov[25] has been successfully employed to investigate the constants of several materials (i.e. Ti[26], Zr[27], Hf[28], c-BN[29]). Here is the brief description of this method.

Consider a crystal compressed by the isotropic pressure P to the density $\rho_1 = 1/V_1$ (where V_1 is the distorted volume from the lattice distortion ε_{ij}). The small homogeneous deformation of this crystal changes each Bravais lattice based vector R to the strained lattice R' in the form of

$$R' = \sum (\delta_{ij} + \varepsilon_{ij}) R_j \quad (1)$$

For a homogeneous strain, the parameters ε_{ij} are simple constants and δ_{ij} is the Kronecher delta. We use the independent strains as shown in Table 1. All these strains are non-volume-conserving. The atomic positions are optimized at all strains. For each strain, several small values of γ are chosen to calculate the total energies E of the strained crystal structure. The calculated E-γ points are fitted to the fourth-order polynomial $E(\rho_1, \gamma)$, eventually the second derivatives of $E(\rho_1, \gamma)$ with respect to γ can be obtained.

Tab. 1 The strains used to calculate the elastic constans for different structures. In the second colunmn, all the unlisted elements of strain tensors are set to zero.

Structure	Distortion	$\frac{1}{V_0}\frac{\partial^2 E}{\partial \delta^2}\Big\vert_{\delta=0}$
C1 and C2	$\varepsilon_{11} = \gamma$	$C_{11} - P$
	$\varepsilon_{13} = \varepsilon_{31} = \gamma$	$4C_{44} - 2P$
	$\varepsilon_{11} = \varepsilon_{22} = \gamma$	$2(C_{11} + C_{12} - P)$
C18	$\varepsilon_{ii} = \gamma, (i = 1,2,3)$	C_{ii}
	$\varepsilon_{23} = \varepsilon_{32} = \gamma$	C_{44}
	$\varepsilon_{13} = \varepsilon_{31} = \gamma$	C_{55}
	$\varepsilon_{12} = \varepsilon_{21} = \gamma$	C_{66}
	$\varepsilon_{22} = \varepsilon_{33} = \gamma$	$\frac{C_{22}}{2} + C_{23} + \frac{C_{33}}{2}$
	$\varepsilon_{11} = \varepsilon_{33} = \gamma$	$\frac{C_{11}}{2} + C_{13} + \frac{C_{33}}{2}$
	$\varepsilon_{11} = \varepsilon_{22} = \gamma$	$\frac{C_{11}}{2} + C_{12} + \frac{C_{22}}{2}$

3 Results and discussion

3.1 Structural and electronic properties

The equilibrium lattice parameter is computed by minimizing the crystal total energy for the different values of lattice constant by means of Murnaghan's equation of state. The structural parameters are listed in Table 2. The value of lattice constant for C1 is about 1.4% higher than the theoretical value[30]. And the same quantity for C2 is about 1.2% higher than theoretical value[12] and 0.06% higher than the available experimental result[3]. Apparently, these values are in consistent with the experiments and previous theoretical calculations.

Tab. 2 The calculated lattice constants (Å), primitive cell volume (Å^3) and bulk modulus (GPa) of PtN_2 at $T = 0$ K and $P = 0$ (GPa), together with the available experimental data and other theoretical results. In the experimental paper[c], two pressure dirivatives were used, giving two bulk moduli.

Structure		a	b	c	β	V_0	B	B'
C1	Present work	5.03				31.84	286	3.27
	GGA[a]	4.96					264	
C2	Present work	4.83				28.20	272	6.50
	GGA[b]	4.86					272	4.96
	LDA[b]	4.77					352	5.02
	Expt.[c]	4.80					354/372	5.26/4
C18	Present work	3.24	4.91	3.77		29.72	612	6.03
	GGA[d]	3.20	4.88	3.78		29.49		
$CoSb_2$	Present work	5.06	4.75	4.98	101.4	29.04	405	10.17
	LDA[e]	4.895	4.833	4.900	99.37	28.5		

续表

	GGA[f]	4.899	4.833	4.899	99.39	28.5		
SH	Present work	2.63		6.15		36.93	93	5.31
	GGA[f]	2.9189		5.0055		36.93		
ST	Present work	4.87	4.87	2.78		33.05	117	4.63
	GGA[f]	4.8238	4.8238	2.8402		33.04		
LS	Present work	2.85	3.77	3.23		34.70	122	4.52
	GGA[f]	2.9021	3.7394	3.1971		34.70		

[a] Ref. [30]

[b] Ref. [12]

[c] Ref. [3]

[d] Ref. [33]

[e] Ref. [37]

[f] Ref. [18]

At some given pressure and temperature, the thermodynamically stable phase is the one with the lowest Gibbs free energy G

$$G = E + PV - TS \quad (2)$$

where E, S, P and V are the internal energy, the vibrational entropy, the pressure and the volume, respectively. The Gibbs free energy G is equivalent to the enthalpy, $H = E + PV$, when our calculation are performed at $T = 0$ K. Therefore, in order to investigate the phase transition, the relationship of enthalpy difference as a function of pressure is shown in Fig. 1. It is noted that no phase transition occurs between different phases in the pressure range studied here. This results are in good agreement with reported in Ref[13, 18]

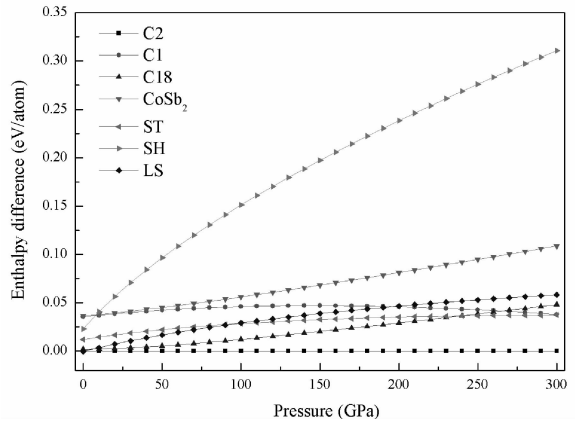

Fig. 1　The Calculated enthalpies as a function of pressure the proposed phases (the enthalpy of C2 phase is set to be zero) at $T = 0$ K.

The total and partial density of states (DOS and PDOS) for the C2 phase are plotted in Fig. 2 at zero pressure and zero temperature. Around Fermi level, DOS decreases to zero at −0.6 eV and is bigger than zero from 0.90 eV, which means that the C2-PtN_2 is a semiconductor with a band gap of 1.5 eV. Given that DFT generally underestimates the band gap often by 30−50%, the true band gap might be located in the region of 2.0−2.3 eV. The valence bands between −6 and −0.6 eV are primarily dominated by 5d states. We can find the hybridization between the 2p state of N and 5d state of Pt lying in the rang from −10 to −0.6 eV, which signifies the strong metal-nonmetal bonding is formed mainly. The 2p state of N contributes mainly to the conduction band.

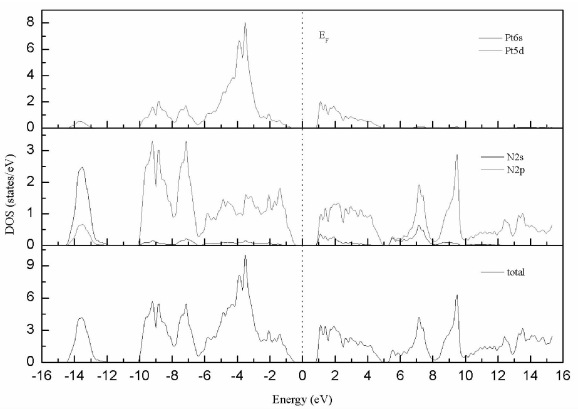

Fig. 2　Calculated partial and total density of states (DOSs) at $T = 0$ K.

In Fig. 3, it shows the DOS is under20, 40, 60 GPa pressure at zero temperature. We can find that the band gap is 1.6eV at 20 GPa, 1.8 eV at 40 GPa and 1.9eV at 60 GPa, respectively, which indicates it increases with pressure. N2s states doped with Pt6s and Pt5d range from −16 eV to −13 eV and move to low energy levels slightly,

which indicates fair locality. The valance band shifts to the low energy region and the conduction band shift to high energy region with increasing pressure, which reveals that the locality strengthens with pressure increasing.

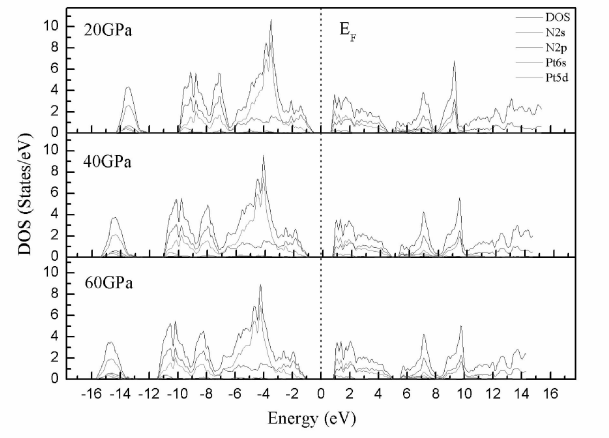

Fig. 3 Partial and total density of states under different pressures at $T=0$ K.

3.2 Elastic properties

The elastic constants of C1, C2, C18 structures at zero temperature and zero pressure are listed in Table 3, along with available experimental data and the previous theoretical values[12, 15, 30]. The elastic constants of C2 phase under high pressures are shown in Fig. 4. This figure indicates that the elastic constants increase monotonically with applied pressure. C_{11} increases dramatically with the applied pressure, while C_{44} increases moderately as well as C_{12}. The criterion for the mechanical stability of crystal structures are expressed by[31]: for cubic structure, $C_{11}>0$, $C_{44}>0$, $C_{11}>|C_{12}|>0$, and $(C_{11}+2C_{12})>0$. These values satisfy these relations for the applied pressures, which guarantee the mechanical stability of PtN_2 under high pressures.

Tab. 3 The elastic constants C_{ij} (GPa), bulk modulus B (GPa), shear modulus G, and Young's modulus Y(GPa) of PtN_2 at $T=0$ K and $P=0$ GPa, together with other theoretical results.

Structure		C_{11}	C_{12}	C_{13}	C_{22}	C_{23}	C_{33}	C_{44}	C_{55}	C_{66}	B	G	Y
C1	Present work	449	176					92			267	108	439
	GGA[a]	457	167					99			264	116	303
C2	Present work	596	86					142			256	180	437
	GGA[b]	668	78					133			272	184	452
C18	Present work	503	157	380	807	143	614	108	330	215			
	GGA[e]	481	111	262	737	107	493	110	266	148	295	187	580

[a] Ref. [30]

[b] Ref. [12]

[e] Ref. [15]

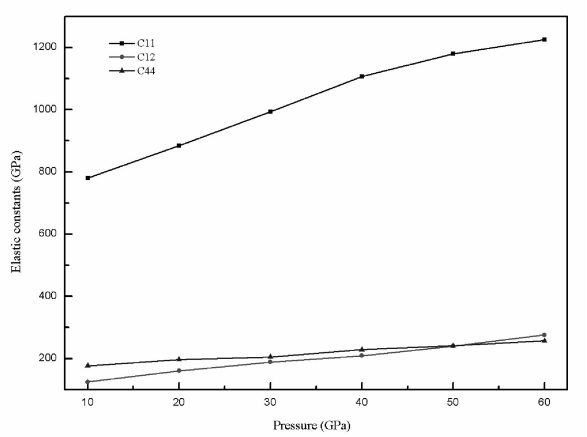

Fig. 4 Calculated pressure dependence of elastic constants for PtN_2 in C2 phase at $T=0$ K.

The Poisson's ratio σ, and Young's modulus Y, which are the most interesting elastic properties for applications, are often measured for polycrystalline materials when we investigate their hardness. These quantities are obtained in terms of the computed data using the following relations

$$\sigma = \frac{3B-2G}{2(3B+G)} \tag{3}$$

$$Y = \frac{9GB}{G+3B} \tag{4}$$

where $G=(G_V+G_R)/2$, $B=(B_V+B_R)/2$ are the shear modulus and bulk modulus according to the Voigt-Reuss-Hill (VRH)[34] average scheme, respectively. G_V and B_V are Voigt's modulus and

G_R, B_R are Reuss's modulus. For cubic phase, they are expressed as

$$G_V = (C_{11} + 3C_{44} - C_{12})/5 \tag{5}$$

$$\frac{5}{G_R} = \frac{4}{(C_{11} - C_{12}) + \frac{3}{C_{44}}} \tag{6}$$

$$B_V = B_R = \frac{(C_{11} + 2C_{12})}{3} \tag{7}$$

Using these relations, the computed bulk modulus, shear modulus, Young's modulus and Poisson's ratio are listed in Table 3, along with the results in Ref.[12,30]. The Poisson's ratio σ under high pressure are given in Table 4. We notice that the Poisson's ratio σ increases moderately with the pressure. It can be noted that Young's modulus shows a linear increase with pressure via observing Fig. 5 as well as bulk modulus and shear modulus.

Tab. 4　The calculated Zener anisotropy(A) factor and Possion ratio(σ) under high pressure.

Pressure(GPa)	10	20	30	40	50	60
A	0.614	0.627	0.602	0.602	0.612	0.644
σ	0.229	0.240	0.240	0.252	0.260	0.265

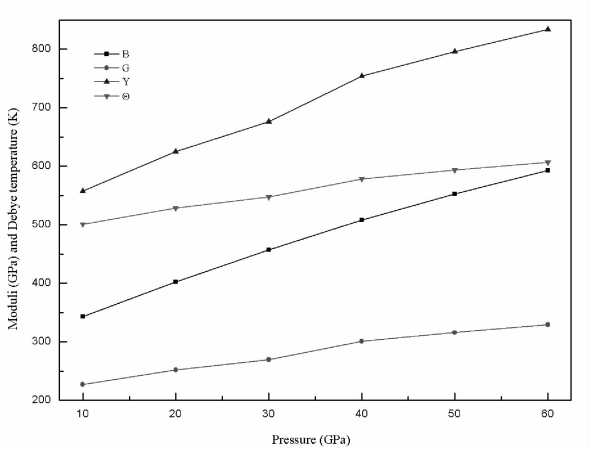

Fig. 5　Calculated pressure dependence of bulk modulus, shear modulus, Young's modulus for C2 phase at T=0 K.

For a cubic crystal, the elastic anisotropy factor A is evaluated by[35]

$$A = \frac{2C_{44} + C_{12}}{C_{11}} \tag{8}$$

For elastically isotropic crystals, anisotropy factor A must be equal to 1, while any deviation from unity corresponds to the degree of elastic anisotropy possessed by the crystal. The obtained A values at 10, 20, 30, 40, 50, 60 GPa are listed in Table 4. We can find that A is almost independent of the pressure and deviates from 1. As we know, the elastic anisotropy is only dependent on the symmetry of the crystal. In other words, the symmetry of C2-PtN_2 stays the same at high pressures.

3.3　Thermodynamic properties

The Debye temperature Θ is used to distinguish between high-and low-temperature regions for a solid. It is closed to the elastic constants, the specific heat, the thermal coefficient, and the melting temperature. If $T > \Theta$, we expect all modes to havea energy levels kBT, if $T < \Theta$, one expects high-frequency modes to be frozen[32]. The Debye temperature Θ can be calculated from the averaged sound velocity υ_m by following equation[36]

$$\Theta = \frac{h}{k_B}\left[\frac{3n}{4\pi}\left(\frac{N_A\rho}{M}\right)\right]^{\frac{1}{3}}\upsilon_m \tag{9}$$

where h is Planck's constant, k_B the Boltzmann's constant, N_A the Avogadro's number, n the number of atoms per formula unit, M the molecular mass per formula unit, ρ ($\rho = M/V$) the density, and the υ_m satisfies the equation

$$\upsilon_m = \left[\frac{1}{3}\left(\frac{2}{\upsilon_s^3} + \frac{1}{\upsilon_p^3}\right)\right]^{\frac{-1}{3}} \tag{10}$$

where υ_s and υ_p are compressional and shear wave velocity, respectively, which are obtained from Navier's equation

$$\upsilon_p = \sqrt{\frac{3B + 4G}{3\rho}}\upsilon_s = \sqrt{\frac{G}{\rho}} \tag{11}$$

In Fig. 5, it is shown that the Debye temperature increases almost linearly with applied pressure, which means there is a change of vibration frequency of particles in C2 phase under pressure. In Fig. 6, there is a moderate increase in the wave velocity. But the Debye temperature and velocity under high pressure are not yet available for comparison.

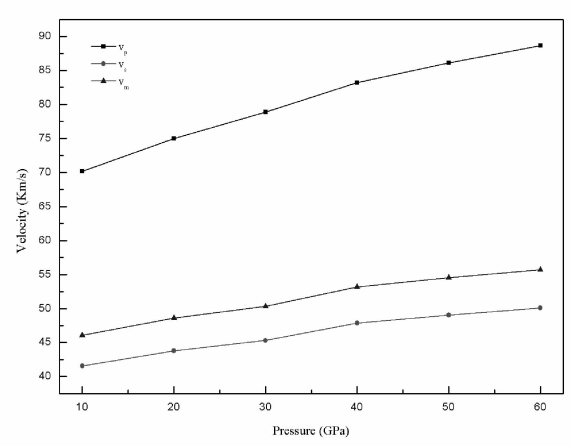

Fig. 6 Predicted wave velocities for C2 phase as a function of pressure at $T=0$ K.

The data of relative volume, thermal expansion and heat capacity are gained through quasi-harmonic Debye model. We plot the curves of the relative volume and pressure at 300, 400, 500, 600 K in Fig. 7. The relative volume decreases with temperature increasing at a constant pressure as the same as the one at a constant temperature. But the influence of pressure is more crucial than temperature. This shows that pressure plays a more essential role in the compressibility of crystal than temperature.

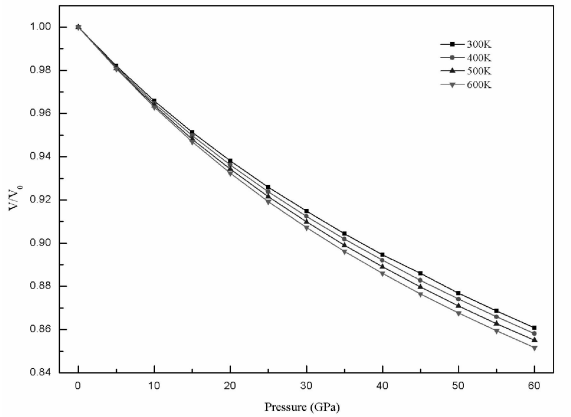

Fig. 7 The relative volume dependence of pressure at different temperatures.

In Fig. 8, we note that the thermal expansion coefficient α decreases with the increase of the pressure at a certain temperature and increases with the increasing temperature at a constant pressure. There is a drastic increment depending the pressure and a tiny increment over temperature at low temperatures. And the rate of change decreases with pressure, which indicates that the temperature dependence of α is a little higher at higher temperatures and higher pressures.

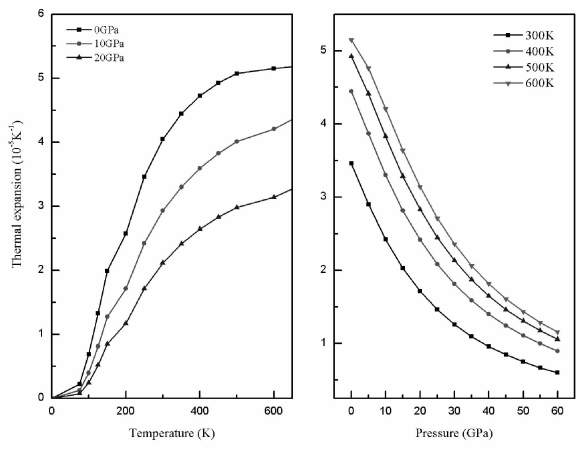

Fig. 8 Temperature and pressure dependence of thermal expansion coefficient under different pressures.

In Fig. 9, the heat capacity changes acutely when the temperature is less than 1300 K because of the anharmonic approximations of the Debye model. However, at higher temperatures and higher pressures, the heat capacity approach to the Dulong-Petit limit (about 74.8 $Jmol^{-1}K^{-1}$), which is common to all solids at high temperatures.

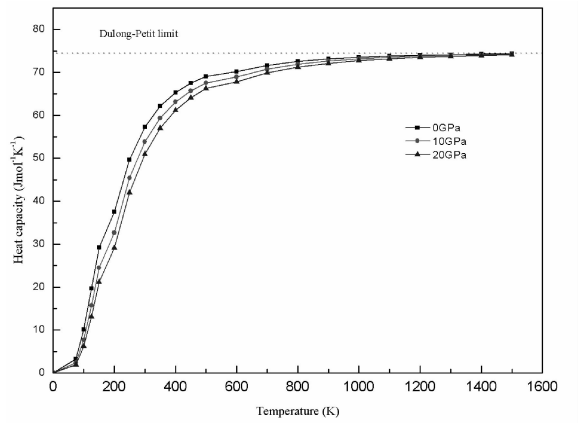

Fig. 9 Temperature dependence of the heat capacity under different pressures.

4 Conclusions

We have some theoretical results on the structural, elastic, electronic, and thermodynamic properties for the PtN_2 based on the DFT. The estimated lattice constant is in excellent agreement with the experimental and other theoretical

results. We find there is no phase transition between different structures and the stability of the metastable phases decreases with the pressure. The calculation of C2-PtN_2 DOS shows that the bonding characteristic has a tiny change with the pressure, which indicates the C2-PtN_2 is a semiconductor. The calculated elastic constants, bulk modulus, shear modulus and Young′s modulus have been compared with some other results. It is the first time that this quantities have been calculated under high pressures as the same as the Debye temperature, the wave velocity and the heat capacity. Unfortunately, there is not other experimental and theoretical results which could be compared to the ones calculated by us.

References:

[1] Crowhurst J C, Goncharov A F, Sadigh B, *et al*. Synthesis and characterization of the nitrides of platinum and iridium[J]. Science, 2006, 311: 1275.

[2] Young A F, Sanloup C, Gregoryanz E, *et al*. Synthesis of novel transition metal nitrides IrN_2 and OsN_2[J]. Phys Rev Lett, 2006, 96(15): 155501.

[3] Gregoryanz E, Sanloup C, Somayazulu M, *et al*. Synthesis and characterization of a binary noble metal nitride[J]. Nature Materials, 2004, 3(5): 294.

[4] Wu Z, Chen X J, Struzhkin V V, *et al*. Trends in elasticity and electronic structure of transition-metal nitrides and carbides from first principles[J]. Phys Rev B, 2005, 71(21): 214103.

[5] Pierson H O. Handbook of refractory oarbides and nitrides: properties, characteristics, processing and applications[M]. William Andrew/Noyes, 1996.

[6] Wang Y X, Arai M, Sasaki T, *et al*. Ab initio study of monoclinic iridium nitride as a high bulk modulus compound[J]. Phys Rev B, 2007, 75(10): 104110.

[7] Leger J M, Djemia P, Ganot F, *et al*. Hardness and elasticity in cubic ruthenium dioxide[J]. Appl Phys Lett, 2001, 79(14): 2169.

[8] Fan C Z, Sun L L, Wang Y X, *et al*. Low compressible noble metal carbides with rock-salt structure: ab initio total energy calculations of the elastic stability[J]. Chin Phys Lett, 2005,22: 2637

[9] Mattesini M, Ahuja R, Johansson B. Cubic Hf_3N_4 and Zr_3N_4: A class of hard materials[J]. Phys Rev B, 2003, 68(18): 184108.

[10] Sahu B R, Kleinman L. PtN: A zinc-blende metallic transition-metal compound[J]. Phys Rev B, 2005, 71(4): 041101.

[11] Patil S K R, Khare S V, Tuttle B R, *et al*. Mechanical stability of possible structures of PtN investigated using first-principles calculations[J]. Phys Rev B, 2006, 73(10): 104118.

[12] Yu R, Zhan Q, Zhang X F. Elastic stability and electronic structure of pyrite type PtN 2: a hard semiconductor [J]. Appl Phys Lett, 2006, 88 (5): 051913.

[13] Chen W, Tse J S, Jiang J Z. An ab initio study of 5d noble metal nitrides: OsN_2, IrN_2, PtN_2 and AuN_2 [J]. Solid State Commun, 2010, 150 (3): 181.

[14] Soto G. Computational of Hf, Ta, W, Re, Ir, Os, and Pt pernitrides[J]. Comput Mater, Sci, 2012, 61:1

[15] Gou H Y, Hou L, Zhang J W. Theoretical hardness of PtN_2 with pyrite[J]. Appl Phys Lett, 2006, 89: 141910.

[16] Fu H Z, Liu W F, Peng F. Theoretical investigtion of structural, elastic and thermodymamic properties for PtN_2 under high pressure [J]. Physica B, 2009, 404: 41.

[17] Åberg D, Sadigh B, Crowhurst J, *et al*. Thermodynamic ground states of platinum metal nitrides[J]. Phys Rev Iett, 2008, 100(9): 095501.

[18] Fan C Z, Li J,. Hu M, *et al*. A Novel layer structuredPtN_2 first principles calculations[J]. Superhard Mater, 2013, 35: 339.

[19] Perdew J P, Burke K, Ernzerhof M. Generalized gradient approximation made simple[J]. Phys Rev Lett, 1996, 77(18): 3865.

[20] Orclejón P, Artacho E and Soler J M. Self-consistent order-N density-functional calculations for very large systems [J]. Phys Rev B, 1996, 53: 10441 (R).

[21] Soler J M, Artacho E, Gale J D, *et al*. The SIESTA method for ab initio order-N materials simulation[J]. J Phys: Conds Matt, 2002, 14(11): 2745.

[22] Sankey O F, Niklewski D J, Drabold D A, et *al*. Molecular-dynamics determination of electronic and vibrational spectra, and equilibrium structures of small Si clusters [J]. Phys Rev B, 1990, 41 (18): 12750.

[23] Troullier N, Martins J L. Efficient pseudopotentials for plane-wave calculations[J]. Phys Rev B, 1991,

43(3): 1993.

[24] Monkhorst H J, Pack J D. Special points for Brillouin-zone integrations[J]. Phys Rev B, 1976, 13(12): 5188.

[25] Sin'Ko G V, Smirnov N A. Ab initio calculations of elastic constants and thermodynamic properties of bcc, fcc, and hcp Al crystals under pressure[J]. Phys: Condens Matt, 2002, 14(29): 6989.

[26] Hao Y J, Zhu J, Zhang L, *et al*. First-principles study of high pressure structure phase transition and elastic properties of titanium[J]. Solid State Sci, 2010, 12(8): 1473.

[27] Hao Y J, Zhang L, Chen X R, *et al*. Phase transition and elastic constants of zirconium from first-principles calculations[J]. J Phys: Cond Matt, 2008, 20(23): 235230.

[28] Hao Y J, Chen X R, Cui H L, *et al*. First-principles calculations of elastic constants of c-BN[J]. Physica B, 2006, 382(1): 118.

[29] Yu R, Zhang X F. Family of noble metal nitrides: First principles calculations of the elastic stability [J]. Phys Rev B, 2005, 72(5): 054103.

[30] Nye J F. Physical properties of Crystals[M]. Oxford: Oxford University Press, 1985.

[31] Christman J R. Fundamentals of Solid State Physics [M]. New York:John Wiley & Sons, 1988.

[32] Chen Z W, Guo X J, Liu Z Y, *et al*. Crystal structure and physical properties of OsN_2 and PtN_2 in the marcasite phase [J]. Phys Rev B, 2007, 75(5): 054103.

[33] Hill R. *Proc. Soc. London. A* 1952, 65: 350.

[34] Ledbetter H M, Moment R L. Elastic properties of face-centered-cubic plutonium [J]. Acta Metal, 1976, 24(10): 891.

[35] Anderson O L, Nafe J E. The bulk modulus - volume relationship for oxide compounds and related geophysical problems[J]. J Geophys Res, 1965, 70(16): 3951.

[36] Yildiz A, Akinci ü, Gülseren O, *et al*. Characterization of platinum nitride from first-principles calculations[J]. J Phys: Condcns Matt, 2009, 21(48): 485403.